

Knockdown of Inwardly Rectifying Potassium Channel Kir2.2 Suppresses Tumorigenesis by Inducing Reactive Oxygen Species–Mediated Cellular Senescence

Inkyoung Lee¹, Chaehwa Park^{1,2}, and Won Ki Kang²

Abstract

Senescence is an important determinant of treatment outcome in cancer therapy. In the present study, we show that knockdown of the inwardly rectifying K⁺ channel Kir2.2 induced growth arrest without additional cellular stress in cancer cells lacking functional p53, p16, and/or Rb. Kir2.2 knockdown also induced senescence-associated β -galactosidase activity and upregulated senescence marker proteins in multiple cancer cell lines derived from different tissues, including prostate, stomach, and breast. Interestingly, knockdown of Kir2.2 induced a significant increase in reactive oxygen species (ROS) that was accompanied by cell cycle arrest, characterized by significant upregulation of p27, with concomitant downregulation of cyclinA, cdc2, and E2F1. Kir2.2 knockdown cells displayed increased levels of PML bodies, DNA damage (γ H2AX) foci, senescence-associated heterochromatin foci, mitochondrial dysfunction, secretory phenotype, and phosphatase inactivation. Conversely, overexpression of Kir2.2 decreased doxorubicin-induced ROS accumulation and cell growth inhibition. Kir2.2 knockdown-induced cellular senescence was blocked by *N*-acetylcysteine, indicating that ROS is a critical mediator of this pathway. *In vivo* tumorigenesis analyses revealed that tumors derived from Kir2.2 knockdown cells were significantly smaller than those derived from control cells ($P < 0.0001$) and showed a remarkable increase in senescence-associated proteins, including senescence-associated β -galactosidase, p27, and plasminogen activator inhibitor-1. Moreover, the preestablished tumors are reduced in size after the injection of siKir2.2 ($P = 0.0095$). Therefore, we propose for the first time that Kir2.2 knockdown induces senescence of cancer cells by a mechanism involving ROS accumulation that requires p27, but not Rb, p53, or p16. *Mol Cancer Ther*; 9(11); 2951–9. ©2010 AACR.

Introduction

Senescence, characterized by specific physiologic and morphologic changes, including reduced proliferation, shortened telomeres, a flat and enlarged cell shape, and the appearance of senescence-associated β -galactosidase (SA- β -Gal) activity, is considered a major determinant of treatment outcome in cancer therapy (1–3). The irreversible growth arrest that manifests during senescence has been associated with cell cycle regulatory tumor suppressors, including p53, Rb, and the cyclin-dependent kinase inhibitors p21^{CIP1}, p27^{Kip1}, and p16^{INK4a} (1, 4–6). In previous studies designed to better understand how malignant

cells escape cellular senescence, we sought to define the genes that control this pathway (7–9). In a cDNA microarray hybridization analysis, we found that doxorubicin-induced senescence selectively inhibited a set of genes that included the inwardly rectifying K⁺ channel Kir2.2.

K⁺ channels have been implicated in a variety of physiologic functions, including proliferation, differentiation, and apoptosis. Pharmacologic evidence indicates that K⁺ channels might be involved in cell cycle and proliferation. The role of K⁺ channels in proliferation has been well documented in many types of normal and malignant cells, including lymphocytes (10), breast cancer cells (11, 12), colon cells (13), and prostate cancer cells (14). Although previous studies have shown that K⁺ channels may be associated with cancer, the precise functions of Kir2.2 in senescence and/or carcinogenesis remain unknown.

In the present study, we explored the role of Kir2.2 in regulating cell cycle arrest and senescence and sought to identify the underlying molecular mechanism. Specifically, we investigated the effects of Kir2.2 expression on the cellular response to doxorubicin in PC-3 human cancer cells. Our results revealed that, even in the presence of an intact pRb pathway, Kir2.2 expression led to decreased senescence and increased doxorubicin resistance.

Authors' Affiliations: ¹Biomedical Research Institute, Samsung Medical Center; ²Department of Medicine, Samsung Medical Center, Sungkyunkwan University School of Medicine, Seoul, Korea

Note: Supplementary material for this article is available at Molecular Cancer Therapeutics Online (<http://mct.aacrjournals.org/>).

Corresponding Authors: Chaehwa Park or Won Ki Kang, Department of Medicine, Samsung Medical Center, Sungkyunkwan University School of Medicine, 50 Irwon-Dong, Seoul, 135-710, Korea. Phone: 82-2-3410-3458, Fax: 82-2-3410-1757. E-mail: cpark@skku.edu or wkkang@skku.edu

doi: 10.1158/1535-7163.MCT-10-0511

©2010 American Association for Cancer Research.

Knockdown of Kir2.2 also upregulated senescence markers in multiple cancer cell lines derived from different tissues. Furthermore, Kir2.2 knockdown increased the levels of p27 and reactive oxygen species (ROS), leading to increases in PML bodies (15), γ H2AX (16), senescence-associated heterochromatin foci (SAHF; ref. 17), interleukin-6 (IL-6), IL-8 (18), and inactivation of both alkaline phosphatase and protein phosphatase 1/2A (19). Conversely, small interfering RNA (siRNA) against p27 (sip27) and the antioxidant *N*-acetylcysteine (NAC) effectively blocked the senescence induced by knockdown of Kir2.2, providing support for the involvement of both p27 and ROS in this pathway. Importantly, we also found that knockdown of Kir2.2 influences tumorigenesis *in vivo*.

Materials and Methods

Cell culture and reagents

Human prostate carcinoma (PC-3, DU145, and LNCaP), gastric carcinoma (MKN74, SNU484, SNU638, and SNU668), and breast cancer (MCF7, SK-BR3, and T47D) cells were grown in RPMI 1640 (Life Technologies Life Science) supplemented with 10% fetal bovine serum, 1 mmol/L NaCO₃, 2 mmol/L L-glutamine, and penicillin-streptomycin. Although these cells were purchased from American Type Culture Collection, no authentication was done by our laboratory. Cells were cultured at 37°C in a humidified 5% CO₂ environment. The 21-nucleotide-long siRNAs targeting Kir2.1, Kir2.2, Kir2.3, Kir2.4, and p27 and negative control siRNA (siC) were purchased from Dharmacon. The full-length Kir2.2 open reading frame was obtained from PC-3 mRNA using a reverse transcription-PCR (RT-PCR)-based cloning technique and inserted into the pCMVTag4C plasmid (Invitrogen). The level of ectopic Kir2.2 expression in stable cell lines was analyzed by immunoblotting using an anti-GFP antibody (Santa Cruz). Cells were transfected with siRNA or plasmids using Effectene (Qiagen) or an Amaxa electroporation system (Amaxa), according to the manufacturer's instructions.

cDNA synthesis and RT-PCR analysis

Total RNA was isolated with the RNeasy mini kit (QIAGEN) and treated with DNase I (QIAGEN). cDNA was generated from total RNA using Moloney murine leukemia virus reverse transcriptase. Plasminogen activator inhibitor-1 (PAI-1), osteonectin, transglutaminase, and the Kir2s were amplified from cDNA by PCR (reaction conditions: 25 cycles of 94°C for 30 seconds, 60°C for 30 seconds, and 72°C for 30 seconds, followed by a final incubation at 72°C for 10 minutes) using primers designed against the coding region of the corresponding human cDNAs (Supplementary Table 1).

Western blot and immunohistochemical analyses

Total cell extracts were obtained using lysis buffer containing 50 mmol/L Tris-HCl (pH 8.0), 150 mmol/L

NaCl, 0.1% SDS, 1% NP40, and 1× protease inhibitors (Roche Applied Science), and protein concentration was determined using the micro-BCA protein reagent (Pierce). Primary antibodies against the following proteins were used: p21 (Santa Cruz), p27 (Santa Cruz), Rb (BD Pharmingen), hypophosphorylated Rb (BD Pharmingen), E2F-1 (Santa Cruz), Cdc2 (Santa Cruz), and β -actin (Sigma). Horseradish peroxidase-conjugated goat anti-rabbit IgG (Santa Cruz) was used as the secondary antibody. Reactive proteins were visualized using an enhanced chemiluminescence kit (Amersham Life Sciences). A streptavidin peroxidase procedure was used for immunohistochemical detection of p27 and PAI-1. Briefly, paraffin-embedded tissue sections were deparaffinized and dehydrated in a graded series of alcohol. Antigenic epitopes were unmasked by autoclaving for 15 minutes in a target retrieval solution (DAKO). p27 and PAI-1 were detected using mouse monoclonal antibodies from Santa Cruz.

Cell growth assessment and colony formation assay

To assess cell numbers, an equal volume of 0.4% (w/v) trypan blue (Sigma) was added to each cell suspension, and viability was determined based on the ability of live cells to exclude the vital dye. Viable cells were counted using a hemocytometer. To measure colony formation, exponentially growing cells were seeded in triplicate in 60-mm-diameter dishes at 2×10^2 per dish. After incubation at 37°C for 2 weeks, cells were stained with 0.005% (w/v) crystal violet. Colonies, defined as cell groups containing a minimum of 50 cells, were counted under a phase contrast microscope.

Cell cycle analysis

For cell cycle analysis, cells were washed twice with ice-cold PBS and then fixed in 2 mL of 70% ethanol. The fixed cells were centrifuged at $200 \times g$ for 10 minutes, and pellets were washed twice with PBS. Cells were then incubated concurrently with 100 μ g/mL propidium iodide (Sigma) and 100 μ g/mL RNase at 37°C for 30 minutes. The percentages of cells in different phases of the cell cycle were measured with a FAC-Star flow cytometer (BD Sciences) and analyzed using Becton Dickinson software (Lysis II, Cellfit).

Fluorescence microscopy

Cells were fixed in 4% (v/v) paraformaldehyde for 15 minutes, washed with PBS, and permeabilized using 0.2% (v/v) Triton X-100 in 3% (w/v) bovine serum albumin (BSA) for 5 minutes. After washing, cells were incubated for 1 hour with either anti- γ H2AX (1:200; Upstate Technology) or anti-PML (1:200; Santa Cruz). Subsequently, cells were washed three times with 3% (w/v) bovine serum albumin in PBS and incubated with Alexa Fluor 488-conjugated secondary antibody (1:5,000) for 1 hour. 4',6-Diamidino-2-phenylindole was added to stain nuclei.

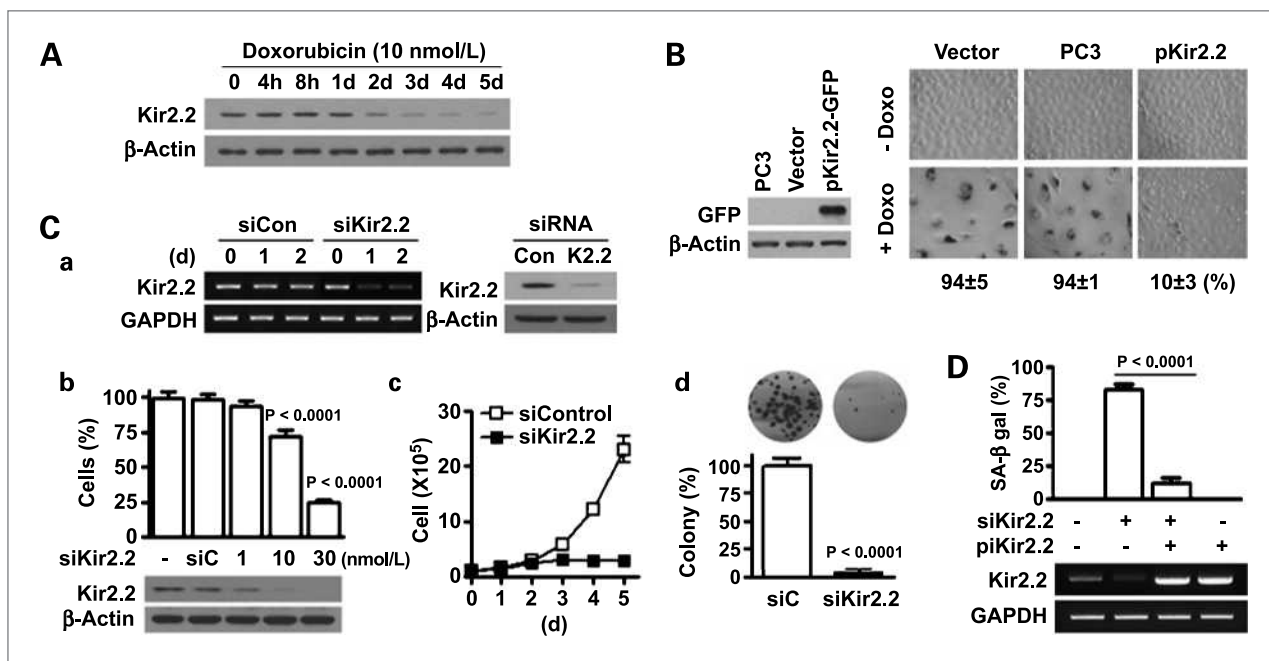


Figure 1. Kir2.2 as a senescence-associated molecular marker. **A**, RT-PCR analysis of Kir2.2 in doxorubicin (10 nmol/L)-treated PC-3 cells. **B**, induction of senescence by low-dose (10 nmol/L) doxorubicin treatment. Left, expression of Kir2.2 in PC-3 cells after transfection of Kir2.2-GFP, as determined by Western blot analysis. Right, after culturing with doxorubicin for 5 d, the cells were stained for SA- β -Gal. The number on the right indicates the percentage of SA- β -Gal-positive cells. **C**, effects of siKir2.2 on the growth of PC-3 cells. **a**, expression of Kir2.2 in PC-3 cells after transfection of siRNAs examined by RT-PCR and Western blot analysis. **b**, siKir2.2 concentration-dependent inhibition of PC-3 cell growth. Cell percentage: viable cell number in test sample/viable cell number in control sample (PBS), 100%. Effects of siKir2.2 (30 nmol/L) versus siC (30 nmol/L) on cell growth kinetics (**c**) and long-term colony formation (**d**). The values represent the means \pm SDs (columns) of three independent experiments (P , siKir2.2 versus siC). **D**, exogenous expression of Kir2.2 (pKir2.2) rescued cells from siKir2.2-induced senescence. The cells were stained for SA- β -Gal activity 5 d after transfection.

Determination of mitochondrial mass, mitochondrial membrane potential, ROS level, and ATP concentration

To measure mitochondrial mass, Mitotracker Red (M7512; Invitrogen) was used. Cells were incubated for 5 minutes with 1 μ mol/L Mitotracker Red, and the intensity of labeling was measured by fluorescence-activated cell sorting (FACS). To assess mitochondrial membrane potential, JC-1 (Molecular Probes) was used; cells were incubated with 10 μ g/mL JC-1 for 10 minutes and washed with HBSS (Life Technologies). To measure intracellular production of ROS, we used two different fluorogenic probes, DCFH-DA and MitoSox (Molecular Probes). DCFH-DA reacts quantitatively with intracellular radicals, being converted to a fluorescent product, 2',7'-dichlorofluorescein (DCF). MitoSox is an indicator of mitochondrial superoxide level and is used to measure mitochondrial ROS production. Stained cells were washed, resuspended in PBS, and analyzed using a FAC-Star flow cytometer (BD Sciences). ATP concentration was determined using an ATP assay kit (FL-ASC; Sigma); the data were normalized to cell number.

Phosphatase assay

All procedures were done as described previously (19). Briefly, pNPP tablets (N-1891; Sigma) were used in the

alkaline phosphatase assay, and phosphatase activity was calculated from a standard curve prepared with *p*-nitrophenol. To determine protein phosphatase 1 and 2A activities, peptide KRpTIRR was used as a substrate and a Malachite Green Assay kit (Upstate Biotechnology) was used. Phosphate released by the enzyme was measured using a standard curve prepared with 0.1 mmol/L KH_2PO_4 .

In vivo tumorigenesis

The effect of Kir2.2 expression on tumor formation was examined by s.c. implanting 1.5×10^6 PC-3 cells into 4-week-old female BALB/c nude mice and monitoring tumor growth every 3 to 4 days using calipers. For a treatment model, exponentially growing PC-3 cells (1.5×10^6 per injection) were implanted s.c. into the nude mice for tumor formation. When tumors reached an average size of 40 to 50 mm^3 (~4 weeks), mice were divided into two groups: siC and siKir2.2. The mice received two times (days 1 and 7) of intratumoral injections of siRNA as a mixture of siRNA (50 nmol/L) in 100 μ L of Effectene per injection. Tumor sizes in two dimensions were measured with calipers, and volumes were calculated with the formula $(a \times b^2) \times 0.5$, wherein *a* is the long axis and *b* is the short axis (in millimeters). All mice were obtained from Charles River Laboratory. Mice were

maintained and sacrificed according to institutional guidelines, and all procedures were approved by the Institutional Committee on the Use and Care of Animals and Recombinant DNA research.

Statistical analysis

Data presented in graphs represent means \pm SDs of values from at least three independent measurements. Differences between two mean values were analyzed using Student's *t* test (paired two-sample *t* test). Differences were considered significant if *P* values were <0.05 .

Results

Kir2.2 level decreases in association with doxorubicin-induced senescence of PC-3 cells

Doxorubicin, a drug frequently used to treat various types of solid tumors, triggers premature senescence (3). Low-dose doxorubicin induced growth arrest in PC-3 human prostate cancer cells, as evidenced by SA- β -Gal-positive cells with a flat, enlarged morphology (7–9). Kir2.2 expression was reduced in response to doxorubicin treatment, with the degree of reduction increasing with the progression of senescence (Fig. 1A). Low-dose doxorubicin induced a senescence-like growth arrest 5 days after the treatment in PC-3 human prostate carcinoma cells (Fig. 1B). However, overexpression of Kir2.2 prevented the doxorubicin-induced growth

arrest compared with doxorubicin-treated control cells. These results indicate that Kir2.2 suppresses DNA damage-induced cell cycle arrest and induction of premature senescence in PC-3 cells. To investigate whether Kir2.2 was directly involved in this drug-induced senescence of PC-3 cells, we examined the effect of Kir2.2 knockdown using siRNA against Kir2.2 (siKir2.2). An analysis of siKir2.2-transfected PC-3 cells showed that Kir2.2 mRNA and protein expression decreased in a siKir2.2-specific manner (Fig. 1C, a), indicating successful knockdown. Figure 1C, b shows that the growth of cancer cells was specifically inhibited by siKir2.2 in a concentration-dependent manner, but not by siC. To explore cell growth in detail, equal numbers of cells were cultured under the same conditions, and changes in cell number were monitored over a 5-day period. As shown in Fig. 1C, c, the numbers of Kir2.2 knockdown cells were significantly less than those of control cells at all time points examined, indicating that knockdown reduced cell growth. Knockdown of Kir2.2 prevented anchorage-independent growth compared with control cells (Fig. 1Cd). Notably, Kir2.2 knockdown induced senescence of carcinoma cells, but not normal prostate epithelial cells (Supplementary Fig. S1). This cell growth inhibition was siKir2.2 dose dependent. As shown in Fig. 1E, Kir2.2 overexpression effectively rescued cells from siKir2.2-induced senescence, indicating that these biological changes were Kir2.2 mediated.

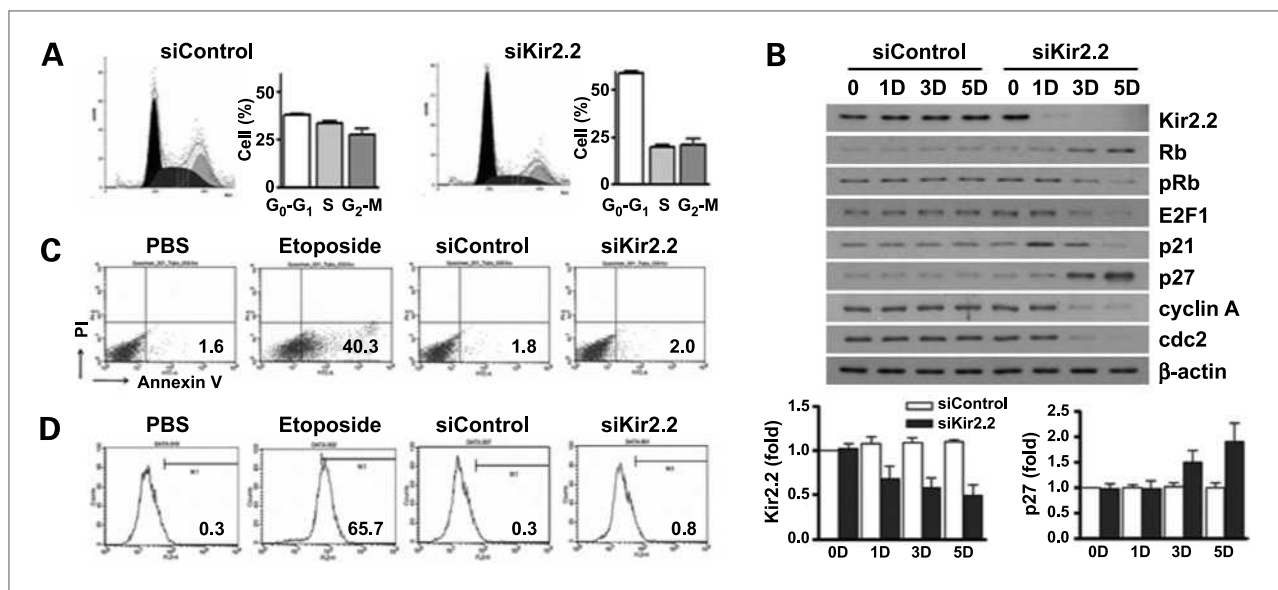


Figure 2. Kir2.2 knockdown induces cell cycle arrest but not cell death. PC-3 cells transfected with siC or siKir2.2 (30 nmol/L) were collected 5 d after transfection and subjected to a flow cytometric analysis. **A**, effect of Kir2.2 knockdown on the cell cycle distribution of PC-3 cells. The results of one representative experiment are presented. The values shown represent the mean \pm SD (columns) of three independent experiments. **B**, changes in the expression of cell cycle-related proteins following siRNA transfection. PC-3 cells were seeded at a concentration of 2×10^5 /mL before siRNA transfection and then harvested at the indicated times. Cell lysates containing 20 μ g of protein were analyzed by SDS-PAGE/Western blotting using the antibodies shown on the right. Bottom, bands on Western blots were quantified by densitometry, and the information is presented in histogram format. Data represent means \pm SDs from three independent experiments. **C**, flow cytometry following Annexin V and propidium iodide staining. **D**, the percentage of terminal deoxynucleotidyl transferase-mediated dUTP nick end labeling-positive cells was determined using flow cytometry. PBS and etoposide (1 μ g/mL for 48 h) were used as negative and positive controls, respectively.

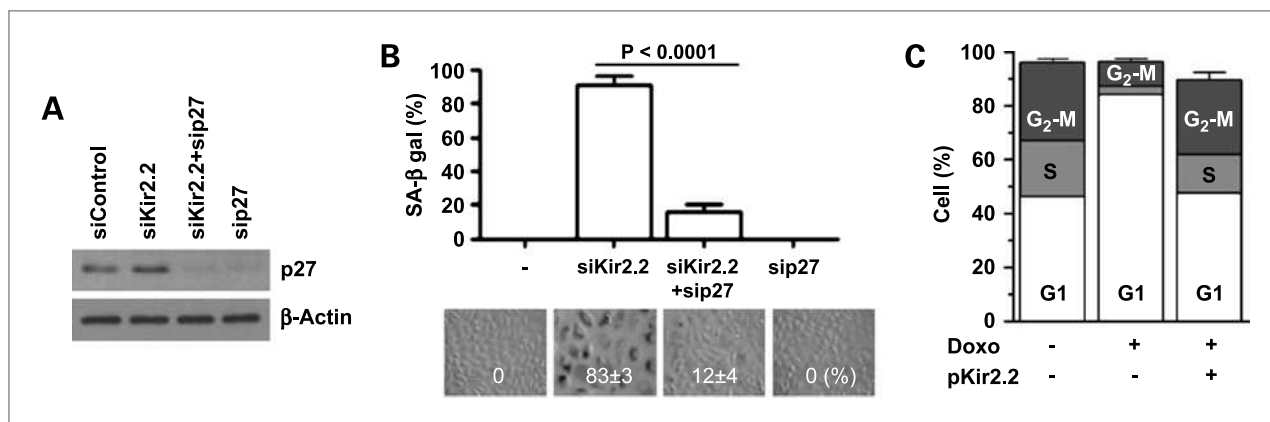


Figure 3. p27 is required for Kir2.2 knockdown-induced senescence. **A**, Western blot analysis of lysates from PC-3 cells transfected with the indicated siRNAs. The day after transfection, cells were analyzed for p27 expression by Western blotting. **B**, knockdown of p27 dramatically decreased the percentage of senescent cells induced by Kir2.2 knockdown from 83 ± 3% to 12 ± 4% ($P < 0.0001$). Cells were scored for SA-β-Gal-positivity (senescence) 5 d after transfection with siRNA. **C**, effect of Kir2.2 expression on the cell cycle of PC-3 cells. Cells were treated with doxorubicin (10 nmol/L) for 5 d and then fixed with 70% ethanol and incubated with RNase A and the DNA-intercalating dye propidium iodide. Results of a representative experiment of three independent experiments are presented.

Kir2.2 knockdown induces p27-mediated cell cycle arrest

As shown in Fig. 1D, knockdown of Kir2.2 significantly arrested cell growth compared with siC-treated PC-3 cells. FACS analysis of siC- and siKir2.2-transfected PC-3 cells on day 5 revealed that siKir2.2-transfected cells were arrested at the G₁ phase of the cell cycle (Fig. 2A). Propidium iodide/Annexin staining (Fig. 2C) and terminal deoxynucleotidyl transferase-mediated dUTP nick end labeling assays (Fig. 2D; Supplementary Fig. S2) confirmed that siKir2.2-transfected cells did not undergo cell death by either apoptosis or necrosis.

Irreversible growth arrest, the defining feature of cellular senescence, is associated with cell cycle inhibitors, including p53, pRb, and the cyclin-dependent kinase inhibitors p21, p27, and p16 (1, 4–6). Therefore, we investigated the effects of Kir2.2 knockdown on the expression levels of cell cycle proteins in PC-3 and MKN74 cells. Consistent with our FACS analysis results, Kir2.2 knockdown increased the levels of the G₁ arrest-inducing protein p27 and decreased cdc2 and E2F1 levels and Rb phosphorylation in both PC-3 (Fig. 2B) and MKN74 (Supplementary Fig. S3).

Kir2.2 expression protects PC-3 cells from doxorubicin-induced growth inhibition

Because Kir2.2 knockdown resulted in increased levels of cell cycle inhibitors, we next examined whether these proteins were required for siKir2.2-induced senescence. More specifically, because p27 expression was enhanced by siKir2.2 in PC-3 and MKN74 cells, we hypothesized that Kir2.2 might modulate senescence-associated cell cycle arrest by regulating p27. Our results revealed that cotransfection with sip27 prevented

accumulation of p27 protein (Fig. 3A) and reduced the SA-β-Gal-positive population in PC-3 cells compared with control cells transfected with siKir2.2 alone (Fig. 3B). These findings suggest that p27 might be essential for the cellular senescence induced by suppression of Kir2.2.

We then attempted to determine whether Kir2.2 overexpression suppresses cell cycle arrest and induction of premature senescence in doxorubicin-treated PC-3 cells. As shown in Fig. 1B, doxorubicin-treated PC-3 cells overexpressing Kir2.2 exhibited improved survival, decreased growth inhibition, and reduced accumulation of SA-β-Gal compared with doxorubicin-treated control PC-3 cells. FACS analyses confirmed that Kir2.2 overexpression relieved doxorubicin-induced cell cycle arrest (Fig. 3C).

siKir2.2 induces senescence in multiple cancer cell lines

The specificity of the senescence-inducing effect of siKir2.2 was tested by evaluating the efficacy of each siKir2.x. RT-PCR analyses confirmed that each siRNA was specific for its respective Kir2.x isoform (Supplementary Fig. S4A). Unlike Kir2.2 knockdown, which induced senescence and SA-β-Gal staining, knockdown of Kir2.1, Kir2.3, or Kir2.4 did not (Supplementary Fig. S4B), indicating that the senescence-inducing effects are specific to knockdown of Kir2.2. To test whether Kir2.2 knockdown-induced senescence is a general phenomenon in cancer cells derived from different tissues, we evaluated the senescence-inducing potential of siKir2.2 in several cell lines (Fig. 4A; Supplementary Fig. S5A). All tested cancer cells from different tumor tissues, including prostate (PC-3, DU145, and LNCaP), stomach (MKN74, SNU638 and SNU668), and breast (MCF7, SK-BR3, and T47D), displayed cellular enlargement and flattening and were

positive for SA- β -Gal staining following knockdown of Kir2.2, which lasted for up to 10 days (Fig. 4A; Supplementary Fig. S5B).

Previously, we reported that doxorubicin induces senescence in PC-3 and LNCaP cells, but not in DU145 cells (7, 9). However, DU145 cells, which contain mutated forms of p53, pRb, and p16, developed senescence in response to Kir2.2 knockdown, indicating that the senescence induced by Kir2.2 knockdown is independent of these tumor suppressors. As shown in Fig. 4B, previously reported senescence marker proteins (9, 20), including PAI-1, osteonectin, and transglutaminase, were induced after Kir2.2 knockdown in the tested cancer cells. Kir2.2 knockdown resulted in mitochondrial dysfunction (21), including an increase in mitochondrial mass, elevated mitochondrial ROS production, and dramatic decreases in both ATP level and mitochondrial membrane potential (Fig. 4C, a). As shown in Fig. 4C, b-d, the cells also exhibited other senescence-associated properties, including increases in PML bodies, γ H2AX, SAHF, IL-6, IL-8, and inactivation of both alkaline phosphatase and protein phosphatase 1/2A.

ROS is a critical mediator of Kir2.2 knockdown-induced senescence in PC-3 cells

Because ROS accumulation induces senescence (22), we tested whether ROS generation might be involved in Kir2.2 knockdown-induced senescence. We measured the intracellular levels of ROS in PC-3 cells by staining with DCFH-DA, a fluorescent marker of cellular oxidant production (23). Figure 5A shows that Kir2.2 knockdown induced ROS accumulation. Rescue of Kir2.2 levels by Kir2.2 overexpression restored intracellular ROS to levels comparable with those in controls, indicating that the accumulation of ROS was directly dependent on the level of Kir2.2. Interestingly, ROS production in response to doxorubicin was significantly decreased by transient overexpression of Kir2.2. Taken together with previous reports that doxorubicin generates ROS (24, 25), these results suggest that Kir2.2 likely blocks chemotherapeutic agent-induced senescence by inhibiting ROS generation.

Inhibition of ROS accumulation has been previously shown to protect against senescence (26). To determine whether accumulation of ROS plays a critical role in Kir2.2 knockdown-induced senescence, we blocked

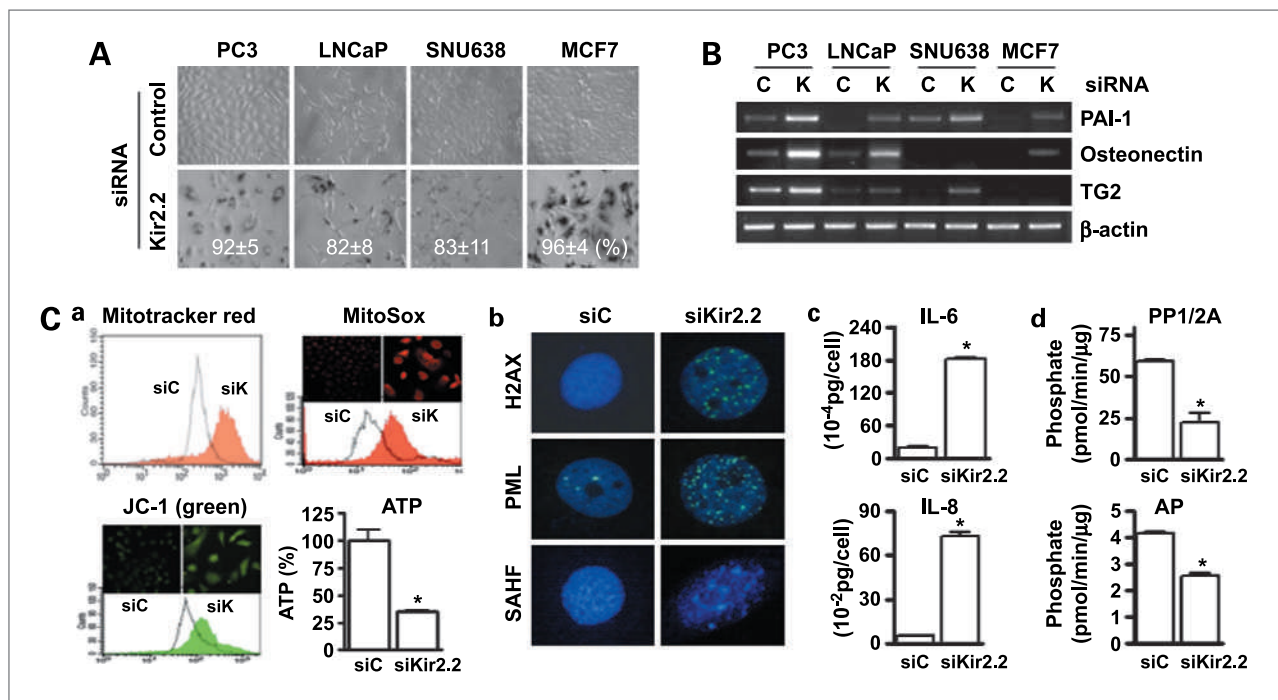


Figure 4. siKir2.2 induces senescence in multiple cancer cell lines. **A**, PC-3, LNCaP, SNU638, and MCF7 cells were stained for SA- β -Gal 5 d after transfection with siRNAs (50 nmol/L). The number indicates the percentage of SA- β -Gal-positive cells. **B**, RT-PCR analysis of senescence-associated genes in multiple cancer cells using primers described previously (20). **C**, induction of senescence-associated markers after transfection of PC-3 cells with the indicated siRNAs (20 nmol/L). siC, siControl; siK, siKir2.2. **a**, mitochondrial dysfunction. Top left, fluorescence of cells on flow cytometry after staining with Mitotracker Red (Invitrogen, M7512), which permits estimation of mitochondrial mass within cells. Top right, MitoSox fluorescence. MitoSox is an indicator of mitochondrial superoxide level and therefore a measure of mitochondrial ROS. Bottom left, JC-1 fluorescence. An increase in green fluorescence indicates mitochondrial membrane depolarization. Bottom right, ATP content in whole cells. **b**, immunofluorescence of γ H2AX, SAHF, or PML bodies. **c**, estimation of IL-6 and IL-8 levels in the medium. An ELISA kit (R&D Systems) was used; data were normalized to cell number (pg secreted protein per cell per day). **d**, Significant inactivation of phosphatase. Top, PP1/2A activity. Bottom, alkaline phosphatase activity. The data were normalized to protein amount (pmol phosphate/ μ g protein/min). *, $P < 0.05$; comparison between siC and siKir2.2 cells.

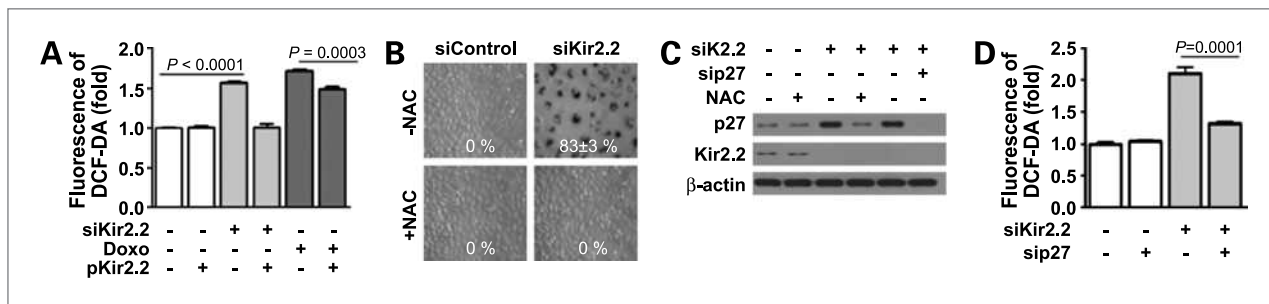


Figure 5. Kir2.2 knockdown induces senescence by increasing ROS accumulation in PC-3 cells. **A**, Kir2.2 knockdown induced an increase in ROS accumulation. DCF fluorescence (fold) indicates ROS generation. **B**, the antioxidant NAC (5 mmol/L) blocked siKir2.2-induced senescence. PC-3 cells were stained for SA-β-Gal 5 d after the transfection of siRNAs (50 nmol/L). The number indicates the percentage of SA-β-Gal-positive cells. **C**, p27 is required for Kir2.2 knockdown-induced ROS generation, and p27 is not synthesized in the absence of ROS, under the same conditions. Western blot analysis of lysates from PC-3 cells transfected with the indicated siRNAs with or without NAC (5 mmol/L). The day after transfection, cells were analyzed for p27 and Kir2.2 expression by Western blotting. **D**, knockdown of p27 dramatically decreased ROS generation induced by Kir2.2 knockdown ($P = 0.0001$). ROS levels were analyzed using the fluorescent dye DCF-DA 5 d after transfection with siRNA.

ROS accumulation with the direct ROS scavenger NAC (27). As shown in Fig. 5B, preincubation with 5 mmol/L NAC prevented the appearance of the senescent phenotype in the Kir2.2 knockdown cells, indicating that senescence induction was caused by ROS accumulation. We tested whether p27 was required for ROS generation induced by Kir2.2 knockdown and whether ROS expression was necessary for the Kir2.2 knockdown-induced increase in p27 levels. As shown in Fig. 5C and D, p27 knockdown decreased ROS generation and the ROS scavenger NAC prevented p27 synthesis in PC-3 cells after transfection of siKir2.2. Therefore, p27 induction may be caused by ROS but induced p27 further contributes to ROS synthesis.

Interestingly, BaCl₂, a well-characterized inhibitor of inwardly rectifying potassium channels, did not affect cell growth (Supplementary Fig. S6A). Also, as shown in Supplementary Fig. S6B, increasing the concentration of potassium in the medium had no effect on doxorubicin-induced cellular senescence. Taken together, these results suggest that potassium transport may not be involved in the modulation of senescence by Kir2.2.

Kir2.2 knockdown decreases *in vivo* tumorigenicity

Finally, we investigated whether Kir2.2 knockdown suppresses tumorigenesis *in vivo*. S.c. transplantation of siC-transfected PC-3 cells into athymic nude mice ($n = 10$) gave rise to tumors with an average size of $289 \pm 39 \text{ mm}^3$ over 41 days. In contrast, athymic mice transplanted with siKir2.2-transfected cells developed tumors that averaged $64 \pm 18 \text{ mm}^3$ in size during the same period ($P < 0.0001$; Fig. 6A), showing that Kir2.2 expression could indeed affect *in vivo* tumor development. More interestingly, in a tumor treatment model the preestablished tumors progressed much more slowly after two times of siKir2.2 injections, which has been introduced directly into the tumors ($P = 0.0095$, *t* test), which strongly suggested that Kir2.2 could be an effective molecular target for cancer therapy (Fig. 6B).

Kir2.2 knockdown induced senescence in these tumors, as evidenced by SA-β-Gal staining (Fig. 6C). An immunohistochemical analysis of paraffin-embedded resected tumors showed strong staining for p27 in siKir2.2-transfected tumors but not in siC tumors (Fig. 6C), consistent with the critical role of p27 in siKir2.2-induced senescence shown in cell culture experiments (see Figs. 2 and 3). A similar staining pattern was observed for the senescence-associated protein PAI-1 (Fig. 6C). Staining for the cell proliferation marker Ki67 clearly showed that cell growth was significantly reduced after Kir2.2 knockdown (Fig. 6C). However, we cannot rule out the possibility that secretory products from senescent cells may have a pro-senescent effect in the whole tumor.

Discussion

Senescence or irreversible growth arrest is considered an important determinant of treatment outcome in cancer therapy (1–4). In a previous cDNA microarray analysis designed to identify growth arrest-associated genes that might contribute to the molecular mechanisms that allow malignant cells to escape senescence, we found that Kir2.2 was selectively downregulated in association with doxorubicin-induced cell growth arrest. Here, we found that Kir2.2 knockdown alone induced senescence-like cell cycle arrest in a variety of cancer cell lines, including those established from prostate (PC-3, DU145, and LNCaP), stomach (MKN74, SNU638 and SNU668), and breast (MCF7, SK-BR3, and T47D).

Kir2.2 knockdown resulted in senescence-induced mitochondrial dysfunction (21), including increases in mitochondrial mass and ROS production and decreases in ATP level and mitochondrial membrane potential. Senescent cells also showed other distinctive properties, including increases in PML bodies (15), DNA damage-associated γH2AX foci (16), SAHF (17), secretory phenotype (18), and phosphatase inactivation (19).

ROS modulates the expression of cell cycle genes and is involved in senescence (22, 28–30). Because we found that doxorubicin induces Kir2.2 downregulation and ROS accumulation in PC-3 cells, we hypothesized that Kir2.2 knockdown-induced senescence might be mediated by ROS. Three lines of evidence indicate that ROS accumulation in response to Kir2.2 knockdown was responsible for causing the cell cycle arrest. First, the antioxidant NAC (27) blocked ROS accumulation in response to Kir2.2 knockdown. Second, NAC inhibited SA- β -Gal staining of Kir2.2 knockdown cells and protected cells from the irreversible growth arrest induced by Kir2.2 knockdown. Third, overexpression of Kir2.2 significantly decreased doxorubicin-induced ROS accumulation. Although K⁺ channels have been previously implicated in cancer (10–14, 31, 32), this is the first study to show that the inwardly rectifying potassium channel Kir2.2 is capable of modulating ROS accumulation and cell cycle arrest.

Cellular senescence/irreversible growth arrest has been associated with induction of tumor suppressors, such as p53, pRb, and p16. In a previous report, Macip et al. (26) suggested that prolonged expression of the tumor suppressors p16 and p21 acts through ROS accumulation to induce permanent growth arrest/senescence. However, we found that Rb, p53, and p16 were dispensable for siKir2.2-induced cell cycle arrest. Among the tested cell lines, both doxorubicin-resistant DU145 cells, which contain mutations in p53, pRb, and p16, and PC-3 cells, which do not have functional p53 or p16, entered senescence following Kir2.2 knockdown. Additionally, we showed that knockdown of p27 by sip27 prevented siKir2.2-induced senescence, supporting the notion that p27 plays a critical role in the induction or maintenance of cellular senescence. This is consistent with previous studies showing that p27, a cyclin-dependent kinase 2 inhibitor, is linked to cell cycle arrest and premature senescence (6, 33). The present results suggest that both p27-mediated growth inhibition and ROS accumulation

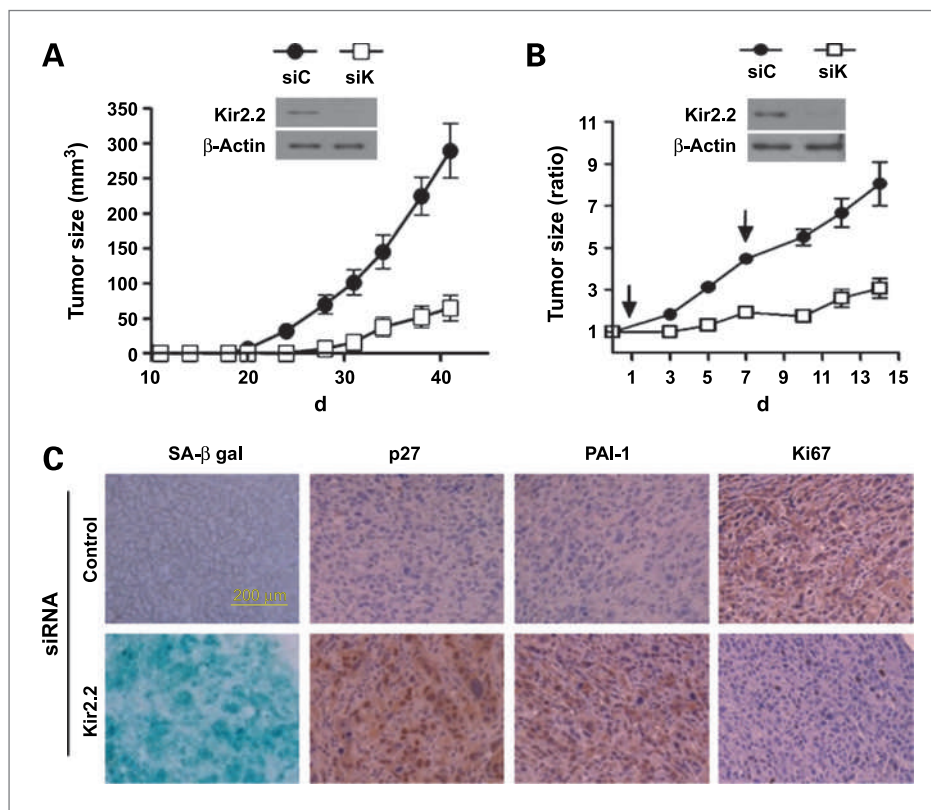


Figure 6. Kir2.2 knockdown decreases *in vivo* tumorigenesis. A, siRNA (50 nmol/L) against Kir2.2 suppresses tumor growth in nude mice. For each injection, 1.5×10^6 PC-3 cells were transfected with siC or siKir2.2 and implanted s.c. into the flanks of 5-wk-old female athymic nu/nu mice. Top, Western blot shows Kir2.2 expression in representative samples. Bottom, gross tumors representative of groups immediately after resection. Day 41 siKir2.2 xenografts were strikingly smaller than siC xenografts ($P < 0.0001$, $n = 10$ mice per group; t test). Points, SEM. B, effect of intratumoral siKir2.2 injection on the growth of established tumors. When tumors reached an average size of 40 to 50 mm³ (~4 wk), the mice received two times (days 1 and 7) of intratumoral injections of siRNA as a mixture of siRNA (50 nmol/L) in 100 μ L of Effectene per injection ($n = 10$). Points, SEM. The top Western blot shows Kir2.2 expression levels in representative samples 2 d after siRNA injection. C, immunohistochemical staining of sections from formalin-fixed, paraffin-embedded tumor samples (resected on postimplantation day 41) showed intense p27 and PAI-1 immunoreactivity, but reduced Ki67 staining, in cells from siKir2.2-transfected tumors. SA- β -Gal staining of fresh tumor tissue 5 d after siRNA injection revealed Kir2.2 knockdown-induced senescence.

contribute to the irreversible growth arrest/senescence induced by Kir2.2 knockdown. Our findings also indicate that cells with increased Kir2.2 expression are resistant to growth arrest and are able to proliferate in the presence of DNA-damaging agents that would normally induce senescence.

In summary, we herein show for the first time that knockdown of Kir2.2 increases p27 levels and ROS accumulation, thereby inducing cellular senescence. This finding is especially significant because our results suggest that Kir2.2 plays a role in the escape from premature senescence of cancer cells and tumor formation *in vivo*.

References

- Schmitt CA, Fridman JS, Yang M, et al. A senescence program controlled by p53 and p16INK4a contributes to the outcome of cancer therapy. *Cell* 2002;109:335–46.
- Roninson IB. Tumor cell senescence in cancer treatment. *Cancer Res* 2003;63:2705–15.
- te Poele RH, Okorokov AL, Jardine L, Cummings J, Joel SP. DNA damage is able to induce senescence in tumor cells *in vitro* and *in vivo*. *Cancer Res* 2002;62:1876–83.
- Chang BD, Xuan Y, Broude EV. Role of p53 and p21waf1/cip1 in senescence-like terminal proliferation arrest induced in human tumor cells by chemotherapeutic drugs. *Oncogene* 1999;18:4808–18.
- Hara E, Smith R, Parry D, Tahara H, Stone S, Peters G. Regulation of p16CDKN2 expression and its implications for cell immortalization and senescence. *Mol Cell Biol* 1996;16:859–67.
- Alexander K, Hinds PW. Requirement for p27(KIP1) in retinoblastoma protein-mediated senescence. *Mol Cell Biol* 2001;21:3616–31.
- Park C, Lee I, Kang WK. E2F-1 is a critical modulator of cellular senescence in human cancer. *Int J Mol Med* 2006;17:715–20.
- Park C, Lee I, Kang WK. Influence of small interfering RNA corresponding to ets homologous factor on senescence-associated modulation of prostate carcinogenesis. *Mol Cancer Ther* 2006;5:3191–6.
- Lee I, Yeom S-Y, Lee S, Kang WK, Park C. A novel senescence-evasion mechanism involving Grap2 and cyclin D interacting protein inactivation by Ras associated with diabetes in cancer cells under doxorubicin treatment. *Cancer Res* 2010;70:1–9.
- Wang YF, Jia H, Walker AM, Cukierman S. K⁺-current mediation of prolactin-induced proliferation of malignant (Nb2) lymphocytes. *J Cell Physiol* 1992;152:185–9.
- Ouadid-Ahidouch H, Roudbaraki M, Ahidouch A, Delcourt P, Prevarskaya N. Cell-cycle-dependent expression of the large Ca²⁺-activated K⁺ channels in breast cancer cells. *Biochem Biophys Res Commun* 2004;316:224–51.
- Ouadid-Ahidouch H, Chaussade F, Roudbaraki M, et al. KV1.1 K(+) channels identification in human breast carcinoma cells: involvement in cell proliferation. *Biochem Biophys Res Commun* 2000;278:272–7.
- Yao X, Kwan HY. Activity of voltage-gated K⁺ channels is associated with cell proliferation and Ca²⁺ influx in carcinoma cells of colon cancer. *Life Sci* 1999;65:55–62.
- Skryma RN, Prevarskaya NB, Dufy-Barbe L, Odessa MF, Audin J, Dufy B. Potassium conductance in the androgen-sensitive prostate cancer cell line, LNCaP: involvement in cell proliferation. *Prostate* 1997;33:112–22.
- Ferbeyre G, de Stanchina E, Querido E, Baptiste N, Prives C, Lowe SW. PML is induced by oncogenic ras and promotes premature senescence. *Genes Dev* 2000;14:2015–27.
- Zhou C, Li Z, Diao H, et al. DNA damage evaluated by γH2AX foci formation by a selective group of chemical/physical stressors. *Mutat Res* 2006;604:8–18.
- Narita M, Nunez S, Heard E, et al. Rb-mediated heterochromatin

Disclosure of Potential Conflicts of Interest

No potential conflicts of interest were disclosed.

Grant Support

Samsung Biomedical Research Institute grant C-A8-201-1 and Korea Research Foundation grant KRF-2008-E00058.

The costs of publication of this article were defrayed in part by the payment of page charges. This article must therefore be hereby marked *advertisement* in accordance with 18 U.S.C. Section 1734 solely to indicate this fact.

Received 06/03/2010; revised 08/25/2010; accepted 09/03/2010; published OnlineFirst 09/14/2010.

- formation and silencing of E2F target genes during cellular senescence. *Cell* 2003;113:703–16.
- Kuilman T, Peeper DS. Senescence-messaging secretome: SMS-ing cellular stress. *Nat Rev Cancer* 2009;9:81–94.
- Kim HS, Song MC, Kwak IH, Park TJ, Lim IK. Constitutive induction of p-Erk1/2 accompanied by reduced activities of protein phosphatases 1 and 2A and MKP3 due to reactive oxygen species during cellular senescence. *J Biol Chem* 2003;278:37497–510.
- Dimri GP, Lee X, Basile G. A biomarker that identifies senescent human cells in culture and in aging skin *in vivo*. *Proc Natl Acad Sci U S A* 1995;92:9363–7.
- Moiseeva O, Bourdeau V, Roux A, Deschênes-Simard X, Ferbeyre G. Mitochondrial dysfunction contributes to oncogene-induced senescence. *Mol Cell Biol* 2009;29:4495–507.
- Chen Q, Ann F, Joshua DR, Yan L-J, Bruce NA. Oxidative DNA damage and senescence of human diploid fibroblast cells. *Proc Natl Acad Sci U S A* 1995;92:4337–41.
- Royall JA, Ischiropoulos H. Evolution of 2',7'-dichlorofluorescein and dihydrorhodamine 123 as fluorescent probes for intracellular H₂O₂ in cultured endothelial cells. *Arch Biochem Biophys* 1993;302:348–55.
- Muller I, Niethammer D, Bruchelt G. Anthracycline-derived chemotherapeutics in apoptosis and free radical cytotoxicity. *Int J Mol Med* 1998;1:491–4.
- Tsang WP, Chau Sophia PY, Kong SK, Fung KP, Kwok TT. Reactive oxygen species mediate doxorubicin induced p53-independent apoptosis. *Life Sci* 2003;73:2047–58.
- Macip S, Igarashi M, Fang L, et al. Inhibition of p21-mediated ROS accumulation can rescue p21-induced senescence. *EMBO J* 2002;21:2180–8.
- Staal FJ, Roederer M, Herzenberg LA. Intracellular thiols regulate activation of nuclear factor κ B and transcription of human immunodeficiency virus. *Proc Natl Acad Sci U S A* 1990;87:9943–7.
- Ames BN, Shigenaga MK, Hagen TM. Oxidants, antioxidants, and the degenerative diseases of aging. *Proc Natl Acad Sci U S A* 1993;90:7915–22.
- Beckman KB, Ames BN. The free radical theory of aging matures. *Physiol Rev* 1998;78:547–81.
- Finkel T, Holbrook NJ. Oxidants, oxidative stress and the biology of ageing. *Nature* 2000;408:239–47.
- Rane SG. Ion channels as physiological effectors for growth factor receptor and Ras/ERK signaling pathways. *Adv Second Messenger Phosphoprotein Res* 1999;33:107–27.
- Chittajallu R, Chen Y, Wang H, Yuan X, Ghiani CA, Heckman T. Regulation of Kv1 subunit expression in oligodendrocyte progenitor cells and their role in G₁-S phase progression of the cell cycle. *Proc Natl Acad Sci U S A* 2002;99:2350–5.
- Collado M, Medema RH, Garcia-Cao I. Inhibition of the phosphoinositide 3-kinase pathway induces a senescence-like arrest mediated by p27Kip1. *J Biol Chem* 2000;275:21960–8.

Molecular Cancer Therapeutics

Knockdown of Inwardly Rectifying Potassium Channel Kir2.2 Suppresses Tumorigenesis by Inducing Reactive Oxygen Species–Mediated Cellular Senescence

Inkyoung Lee, Chaehwa Park and Won Ki Kang

Mol Cancer Ther 2010;9:2951-2959. Published OnlineFirst September 14, 2010.

Updated version Access the most recent version of this article at:
doi:[10.1158/1535-7163.MCT-10-0511](https://doi.org/10.1158/1535-7163.MCT-10-0511)

Supplementary Material Access the most recent supplemental material at:
<http://mct.aacrjournals.org/content/suppl/2010/09/14/1535-7163.MCT-10-0511.DC1>

Cited articles This article cites 33 articles, 16 of which you can access for free at:
<http://mct.aacrjournals.org/content/9/11/2951.full#ref-list-1>

Citing articles This article has been cited by 2 HighWire-hosted articles. Access the articles at:
<http://mct.aacrjournals.org/content/9/11/2951.full#related-urls>

E-mail alerts [Sign up to receive free email-alerts](#) related to this article or journal.

Reprints and Subscriptions To order reprints of this article or to subscribe to the journal, contact the AACR Publications Department at pubs@aacr.org.

Permissions To request permission to re-use all or part of this article, use this link
<http://mct.aacrjournals.org/content/9/11/2951>.
Click on "Request Permissions" which will take you to the Copyright Clearance Center's (CCC) Rightslink site.